Spin Fluctuations in Heisenberg Paramagnets. I. Diagrammatic Expansion for the Moments of the Spectral Density at Finite Temperature*

G. F. Reiter
Department of Physics, University of California, Irvine, California 92664
(Received 23 December 1969; revised manuscript received 23 July 1971)

A diagrammatic method for calculating the moments of the spectral density for the paramagnet is presented. The method yields exact results at infinite temperatures and values for the moments that are correct to lowest order in $1/c$ at finite temperatures, where c is the effective number of spins in the range of the exchange interaction. Explicit formulas for the second and fourth moments for the simple-cubic and body-centered-cubic lattices are presented. It is shown that to lowest order in $1/c$, the moments $\langle\omega^{2n}\rangle_q$ are proportional to $[\frac{1}{3}S(S+1)]^n$, with the constants of proportionality independent of spin. As a consequence, there is a simple "law of corresponding states" relating the spectral densities for different values of the spin. The resummation of diagrams to obtain self-consistent equations for the spectral density is discussed.

I. INTRODUCTION

The Heisenberg paramagnet is probably the simplest example of a realistic model system that undergoes a phase transition. As such, it provides an opportunity to study in detail the dynamical processes at the critical point, and to investigate the validity of theoretical suggestions as to the nature of these processes, such as the dynamical scaling "laws."[1] Interest in the model is not confined to the critical behavior, however.

Recent NMR and EPR[2] measurements have shown that an accurate treatment of the dynamics at high temperatures compared to the critical temperature is necessary to explain, even qualitatively, the temperature-dependent exchange-narrowed linewidth in materials such as $RbMnF_3$ and MnF_2.[3] Furthermore, neutron scattering data are available at high temperatures on $RbMnF_3$ with which one can compare directly theoretical predictions of the fluctuation spectra.[4,5]

The early theoretical attempts to understand the dynamics were limited to[6,7] semiphenomenological attempts to relate the fluctuation spectra to the first two moments of the spectral density, which could be calculated at $T=\infty$. In addition, numerical calculations have been made of various time-dependent correlation functions by actually solving the many-spin equations of motion for a large array of classical spins on a computer.[4,5,8] In one dimension, numerical calculations have been made for spin $\frac{1}{2}$ for chains of about ten spins by actually finding the eigenvalues of the Hamiltonian.[9] Such approaches do not confront what we take to be the central theoretical task of reducing the many-spin problem to a tractable form on the basis of physically justifiable approximations, so that reasonably accurate values for measured parameters can be calculated and some insight gained into the essential features of the dynamics.

The first attempt in this direction was made by Bennett and Martin.[10] Their results, although in principal capable of describing the complete fluctuation spectrum, were limited to a calculation of the diffusion coefficient, and have never been extended. The approximation that they used has been criticized by Resibois and DeLeneer, who have calculated, using a diagrammatic method, the fluctuation spectra at all wave vectors and frequencies, for $T=\infty$. The latter work has recently been extended to finite temperatures.[11]

Although the work of Resibois and DeLeneer meets in many respects the criterion stated above, the short-wavelength fluctuation spectra predicted by them at $T=\infty$ is, we believe, qualitatively incorrect, and the diagrammatic expansion they have used is unnecessarily complicated.

We have developed an alternative theoretical framework for treating the problem, and introduced, within that framework, approximations that differ in their physical content from those of Resibois and DeLeneer. In the present paper, we derive a diagrammatic expansion for the moments of the spectral density. In a subsequent paper, we shall derive equations of motion that effectively sum infinite subsets of these diagrams, and allow the calculation of most of the measurable dynamical properties of the Heisenberg paramagnet.

In Sec. II, we define the mathematical framework for the calculation, and recall some well-known exact results. In Sec. III we derive an exact diagrammatic expression of the moments at infinite temperatures. In Sec. IV, the derivation is extended to all temperatures above the critical temperature, with the restriction that the moments are evaluated only to lowest order in $1/c$. In Sec. V, we discuss the resummation of diagrams to obtain calculable expressions for the spectral density.

II. MATHEMATICAL PRELIMINARIES

The Heisenberg paramagnet is described by the Heisenberg Hamiltonian,

$$\mathcal{H} = -\tfrac{1}{2}\sum_{i,j} \hbar V_{ij}\vec{S}_i\cdot\vec{S}_j = -\tfrac{1}{2}\sum_q \hbar V(q)\vec{S}(q)\cdot\vec{S}(-q)\ , \tag{2.1}$$

where $\vec{S}_i$ is a spin operator, of magnitude S, associated with the site i of a lattice. The components of the spin operators satisfy the commutation relations

$$\begin{aligned}[S_i^z, S_j^\pm] &= \pm\delta_{ij}S_i^\pm\ ,\\ [S_i^+, S_j^-] &= 2\delta_{ij}S_i^z\ .\end{aligned} \tag{2.2}$$

If $\vec{a}_1$, $\vec{a}_2$, $\vec{a}_3$ are the basis vectors for the primitive cell of the lattice, then we let the operator associated with any site be identical with the operator at the site that is translated by $n\vec{a}_1$, $n\vec{a}_2$, or $n\vec{a}_3$. The operator $\vec{S}(\vec{q})$ is defined as $N^{-1/2}\sum_i e^{-i\vec{q}\cdot\vec{r}_i}\vec{S}_i$, where the summation is over the $N=n^3$ sites of the parallelopiped defined by $(n\vec{a}_1, n\vec{a}_2, n\vec{a}_3)$. The exchange constants V_{ij} can be arbitrary, but depend only on the relative separation $\vec{r}_i-\vec{r}_j$ between sites. $V(q)$ is defined as

$$V(q) = \sum_i e^{-i\vec{q}\cdot(\vec{r}_i-\vec{r}_j)}\ V_{ij}\ .$$

The operators $\vec{S}$ act on the $(2S+1)$-dimensional Hilbert space of spin states, which we denote by H_i. Associated with each such space H_i is the space of all bounded operators on H_i, which we denote by V_i. V_i is of dimension $(2S+1)^2$.

The vector space obtained by taking the tensor product of the V_i for all sites i in the parallelopiped defined previously will be denoted by V. Each element of V_i, say, S_i^z, can be associated with the element of V defined by $I_1\otimes I_2\cdots S_i^z\cdots\otimes I_N$, where I_j is the identity operator on H_j. We will also, for simplicity, denote this element of V by the symbol S_i^z.

The Hamiltonian $\mathcal{H}$, which is itself an element of V, defines a one-parameter Lie group of transformations $\{v_t\}$ that map V onto itself. This transformation is defined by

$$\mathcal{O}(t) \equiv v_t\times\mathcal{O} \equiv e^{i/\hbar\mathcal{H}t}\mathcal{O}e^{-i/\hbar\mathcal{H}t}$$

for any element $\mathcal{O}\in V$. The generator of the group, which we will denote by $\mathcal{L}$, is the Liouville operator for the system. It is an operator from V onto itself. The action of $\mathcal{L}$ on any element $\mathcal{O}\in V$ is explicitly

$$\mathcal{L}\times\mathcal{O} = \frac{1}{\hbar}[\mathcal{O},\mathcal{H}]\ ,$$

where

$$v_t\times\mathcal{O} = e^{-i\mathcal{L}t}\times\mathcal{O}\ .$$

We define the bracket $(\ ,\ )$, which is a function from $V\otimes V$ to the real line, as

$$(A,B) \equiv \langle\langle \int_0^\beta e^{\tau\mathcal{H}}Ae^{-\tau\mathcal{H}}B\,d\tau\rangle\rangle\ . \tag{2.3}$$

The bracket $\langle\langle\ \rangle\rangle$ denotes an average over the canonical ensemble, defined by the density matrix $\rho_{eq}=e^{-\beta\mathcal{H}}/\mathrm{Tr}e^{-\beta\mathcal{H}}$. That is, $\langle\langle\mathcal{O}\rangle\rangle = \mathrm{Tr}\rho_{eq}\mathcal{O}$. The trace, of course, is taken over the states of the Hilbert space H, where H is the direct product of the spaces H_i. It is readily verified that the relation

$$\langle A\,|\,B\rangle \equiv (A^\dagger, B)\ ,$$

where $A^\dagger$ is the adjoint of B defines a complex scalar product on V so that V with this inner product is a Hilbert space. From the cyclic invariance of the trace, it is easy to show that $\mathcal{L}$ is an Hermitian operator in this Hilbert space:

$$\langle A\,|\,\mathcal{L}\times B\rangle = \langle\mathcal{L}\times A\,|\,B\rangle\ .$$

Furthermore, one can readily show that

$$\langle\mathcal{L}\times A\,|B\rangle = \langle\langle[B,A^\dagger]\rangle\rangle\ . \tag{2.4}$$

This last identity indicates that the matrix elements of $\mathcal{L}$ can all be expressed as equilibrium averages.

The linear response of the magnetization to an arbitrary external field, in the paramagnetic regime, is determined by the quantity

$$\Sigma(\vec{q},t) = (S^z(\vec{q},t), S^z(-\vec{q},0)) = \langle S^z(\vec{q},0)\,|\,S^z(\vec{q},t)\rangle\ .$$

$\Sigma(q,0)$ has the physical interpretation of being the isothermal response of the magnetization to a magnetic field of strength $(g\mu_B)^{-1}$ and wave vector $\vec{q}$, and will be denoted by $\chi(\vec{q},0)$. $\Sigma(\vec{q},t)$ describes the decay of the qth component of the magnetization in the absence of any external fields. We shall actually be concerned with the Laplace transform of $\Sigma(\vec{q},t)$,

$$\Sigma(\vec{q},z) = \int_0^\infty e^{izt}\Sigma(\vec{q},t)\,dt,\quad \mathrm{Im}z>0\ .$$

The quantity $\Sigma(\vec{q},z)$ can be related to the dynamical susceptibility, defined as

$$\chi(\vec{q},z) = i\int_0^\infty \langle\langle[S^z(\vec{q},t), S^z(-\vec{q},0)]\rangle\rangle e^{izt}\,dt\ ,$$

$$\mathrm{Im}z>0\ . \tag{2.5}$$

By differentiating the expression for $\Sigma(\vec{q},t)$ with respect to time, we obtain

$$\begin{aligned}\frac{d}{dt}\Sigma(\vec{q},t) &= -i\langle S^z(\vec{q},0)\,|\,\mathcal{L}\times S^z(\vec{q},t)\rangle\\ &= -i\langle\langle[S^z(\vec{q},t), S^z(-\vec{q},0)]\rangle\rangle\ .\end{aligned}$$

Hence

$$\Sigma(\vec{q},z) = [\chi(\vec{q},z)-\chi(\vec{q},0)]/iz\ . \tag{2.6}$$

Utilizing the definition $\vec{S}(\vec{q},t) = e^{-i\mathcal{L}t}\vec{S}(\vec{q})$, we have

$$\Sigma(\vec{q},z) = i\langle S^z(\vec{q})\,|\,(z-\mathcal{L})^{-1}\,|\,S^z(\vec{q})\rangle\ . \tag{2.7}$$

Thus, the response function $\Sigma(\vec{q}, z)$ is a diagonal matrix element of the resolvent operator $(z - \mathcal{L})^{-1}$.

If we introduce the projection operator P onto the subspace of V containing linear combinations of S_i^z, it can be shown[7] that

$$\Sigma(\vec{q}, z) = i \langle S^z(\vec{q}) | S^z(\vec{q}) \rangle [z - \varphi(\vec{q}, z)]^{-1} , \quad (2.8)$$

where

$$\varphi(\vec{q}, z) = \langle (I-P)\mathcal{L}S^z(\vec{q}) | [z - (I-P)\mathcal{L}(I-P)]^{-1} \times | (I-P)\mathcal{L}S^z(\vec{q}) \rangle / \chi(\vec{q}, 0) . \quad (2.9)$$

The projection operator P is explicitly $\sum_q |S^z(\vec{q}, 0)\rangle \times \langle S^z(\vec{q}, 0)| / \chi(\vec{q}, 0)$.

Information about $\Sigma(\vec{q}, z)$ for large z and an expansion of $\Sigma(\vec{q}, t)$ in powers of t may be obtained from the Neumann series for the resolvent operator,

$$(z - \mathcal{L})^{-1} = z^{-1} \sum_{n=0}^{\infty} (z^{-1}\mathcal{L})^n . \quad (2.10)$$

If we insert (2.10) into (2.7) we obtain

$$\Sigma(\vec{q}, z) = i \sum_{n=0}^{\infty} z^{-(n+1)} \langle S^z(\vec{q}) | \mathcal{L}^n | S^z(\vec{q}) \rangle , \quad (2.11)$$

which is the Laplace transform of the expansion in the time domain,

$$\Sigma(\vec{q}, t) = \sum_{n=0}^{\infty} \frac{(-it)^n}{n!} \langle S^z(\vec{q}) | \mathcal{L}^n | S^z(\vec{q}) \rangle . \quad (2.12)$$

From (2.6), we have the relation

$$\mathrm{Re}\Sigma(\vec{q}, \omega + i\epsilon) = \chi''(\vec{q}, \omega)/\omega . \quad (2.13)$$

The real and imaginary parts of $\Sigma(\vec{q}, \omega + i\epsilon)$ are related by the Kramers-Kronig relation, which, in view of (2.13), can be written as

$$\mathrm{Im}\Sigma(\vec{q}, \omega + i\epsilon) = \frac{1}{\pi} \int_{-\infty}^{\infty} \frac{\chi''(\vec{q}, \omega')\, d\omega'}{\omega'(\omega - \omega')} . \quad (2.14)$$

If we expand $(\omega - \omega')^{-1}$ in powers of (ω'/ω), and compare the resultant series with (2.11), we find the expression for the moments of the spectral density, $\chi''(\vec{q}, \omega)/\omega$, which we will denote by $\langle \omega^n \rangle_q$, in terms of matrix elements of the Liouville operator:

$$\langle \omega^n \rangle_q \equiv \frac{1}{\pi} \int_{-\infty}^{\infty} \frac{\omega^{n-1} \chi''(\vec{q}, \omega)\, d\omega}{\chi(\vec{q}, 0)} = \frac{\langle S^z(\vec{q}) | \mathcal{L}^n | S^z(\vec{q}) \rangle}{\chi(\vec{q}, 0)} . \quad (2.15)$$

In fact, the odd moments are all zero, since from (2.4) we have

$$\langle S^z(\vec{q}) | \mathcal{L}^{2n+1} | S^z(\vec{q}) \rangle = \langle\langle [\mathcal{L}^n \times S^z(\vec{q}), (\mathcal{L}^n \times S^z(\vec{q}))^\dagger] \rangle\rangle = (-1)^n \langle\langle [\mathcal{L}^n \times S^z(\vec{q}), \mathcal{L}^n \times S^z(-\vec{q})] \rangle\rangle . \quad (2.16)$$

But the translation and inversion symmetries of the Hamiltonian guarantee that $\langle \omega^n \rangle_q = \langle \omega^n \rangle_{-q}$, whereas the right-hand side of (2.16) is antisymmetric in the exchange of $\vec{q}$, $-\vec{q}$, and hence must vanish. Similarly, we may obtain an expansion of $\varphi(\vec{q}, z)$ for large z, by utilizing the Neumann expansion of $(z - \mathcal{L}')^{-1}$, where $\mathcal{L}' = (I-P)\mathcal{L}(I-P)$. We find that

$$\varphi(\vec{q}, z) = \sum_{n=0}^{\infty} \langle \mathcal{L} \times S^z(\vec{q}) | \mathcal{L}'^{2n} | \mathcal{L} \times S^z(\vec{q}) \rangle z^{-(2n+1)} / \chi(\vec{q}, 0) \equiv \sum_{n=0}^{\infty} \Omega^{2n+2}(\vec{q}) z^{-(2n+1)} . \quad (2.17)$$

It is clear from (2.8) that $\Omega^{2n}(\vec{q})$ and $\langle \omega^{2n} \rangle_q$ are related. In particular, $\langle \omega^2 \rangle_q = \Omega^2(\vec{q})$, $\langle \omega^4 - \langle \omega^2 \rangle^2 \rangle_q = \Omega^4(\vec{q})$. Thus, for large z,

$$\varphi(\vec{q}, z) = \langle \omega^2 \rangle_q / z + \langle \omega^4 - \langle \omega^2 \rangle_q \rangle_q / z^3 + O(1/z^5) . \quad (2.18)$$

Unlike the expansion (2.11), which may not converge for $|z|$ less than the spectral radius of $\mathcal{L}$, the expansion in the time domain converges for all t. In principal then, a calculation of the moments can be used to determine $\Sigma(\vec{q}, t)$. In practice it is difficult to calculate more than the first few moments, so that (2.12) is only useful for short times.

III. DIAGRAMMATIC EXPANSIONS AT INFINITE TEMPERATURE

There are two alternative means of calculating the moments. One can perform explicitly the multiple commutations implied by $\mathcal{L}^{2n}$ using the basic relations (2.2), and evaluate the equilibrium average of the resultant operator. An alternative scheme consists of inserting a complete set of states in V between the factors of $\mathcal{L}$, thus representing the moments as products of matrix elements of $\mathcal{L}$. The first method is the standard means, employed in NMR and EPR studies, for the calculation of the moments, usually at $T = \infty$. The second method leads to graphical expressions for the moments. These have been used extensively by Resibois and DeLeener, for the case of spin $\frac{1}{2}$. Although the derivation employed by these authors is restricted to spin $\frac{1}{2}$, this restriction is not necessary. Diagrammatic expansions can be obtained for arbitrary spin, by the method we will outline. A similar method has been discussed by Wegner.[12]

A complete set of states for the space V_i can be obtained from the $(2S+1)^2$ tensor operators Y_i^{nm}. These can be defined in terms of the spin operators by means of the relation

$$\sum_{m=-n}^{m=n} Y_i^{nm} t^m = \left(\frac{-tS_i^+ + 2S_i^z + S_i^-}{t} \right)^n ,$$

where n runs from 0 to $2S$. Any operator in V_i can

be expressed as a linear combination of these operators, and hence any operator in V is a linear combination of products of these operators. The set of operators one obtains by taking all possible products of the Y_i^{nm} for different i, n, m is therefore complete. One can in general construct from such a set, an orthonormal basis for V. We shall first do this for the case that $T=\infty$, in order to illustrate the graphical method in the simplest case. The inner product reduces to

$$\langle A \mid B \rangle \to \beta \, \mathrm{Tr} A^\dagger B/(2S+1)^N.$$

Since the moments do not depend upon a multiplicative factor in the definition of the inner product, we will simply redefine the inner product at $T=\infty$ ($\beta=0$) to be $\mathrm{Tr}A^\dagger B/(2S+1)^N$, and denote it by $\langle A \mid B \rangle_\infty$. With this definition

$$\langle Y_i^{nm} \mid Y_{i'}^{n'm'} \rangle_\infty = C_{nm} \delta_{ii'} \delta_{nn'} \delta_{mm'} .$$

The constant C_{nm} can be evaluated by the method analogous to that outlined in Erdelyi *et al.*,[13] and is

$$C_{nm} = \frac{(2S+1+n)!\,(n!)^2}{(2n+1)!\,(2S-n)!} \; \frac{2n!}{(n-m)!\,(n+m)!} \Big/ (2S+1) . \tag{3.1}$$

The operators

$$A_i^{nm} \equiv Y_i^{nm}/(C_{nm})^{1/2}$$

are orthonormal. A_i^{00} is independent of i and is simply the identity operator on H. The identity operator on V can be written as

$$I = \mid A^{00} \rangle \langle A^{00} \mid + \sum_i \sum_{n=1}^{2S} \sum_{m=-n}^{m=+n} \mid A_i^{nm} \rangle \langle A_i^{nm} \mid$$

$$+ \sum_{\{i,j\}} \sum_{n=1}^{2S} \sum_{n'=1}^{2S} \sum_{m=-n}^{m=+n} \sum_{m=-n'}^{m=+n'} \mid A_i^{nm} A_j^{n'm'} \rangle$$

$$\times \langle A_i^{nm} A_j^{n'm'} \mid + \cdots . \tag{3.2}$$

The notation $\{i,j\}$ indicates that the sum is to be taken over all distinct pairs, with $i \neq j$. The higher-order terms contain the sum over triplets, etc. To obtain the graphical expansion of $\langle \omega^{2n} \rangle_q$, we insert the identity (4.11) between powers of the operator $\mathcal{L}$. For instance,

$$\langle \omega^2 \rangle_q = N^{-1} \sum_j e^{iq(r_i - r_j)} \sum_{\{A\}} \langle A_i^{10} \mid \mathcal{L} \mid \{A\} \rangle_\infty$$

$$\times \langle \{A\} \mid \mathcal{L} \mid A_j^{10} \rangle_\infty ,$$

where $\{A\}$ denotes the set of all intermediate states.

The intermediate states are represented by lines, labeled with three indices, (i,n,m). The matrix elements of $\mathcal{L}$ are the vertices. As an example, we consider the case that $S=\frac{1}{2}$, which is particularly simple since $n=1$ for all operators. We will denote $A_i^{10} = S_i^z / [\frac{1}{3}S(S+1)]^{1/2}$ by a dotted line, and $A_i^{1\pm1} = \mp S_i^\pm / [\frac{2}{3}S(S+1)]^{1/2}$ by lines with arrows, an arrow to the left signifying S^+, an arrow to the right, S^-. For simplicity, we will suppress the index n, and redefine $A_i^{+1} = S^+ / [\frac{2}{3}S(S+1)]^{1/2}$. The basic vertices, from which all the graphs are composed, are particular matrix elements of $\mathcal{L}$ and are shown in Fig. 1. More general matrix elements consist of a basic vertex together with lines representing the same operator in the initial and final state as in Fig. 2. The total contribution to $\langle A_i^0 \mid \mathcal{L}^{2n} \mid A_j^0 \rangle$ consists of all the distinct graphs that can be drawn using $2n$ basic vertices, beginning with a dotted line at the left at site i, and ending with a dotted line at site j. Graphs which differ only in the sequence, from left to right, that the vertices appear, are counted as distinct. The contribution for a particular graph is obtained by multiplying all the terms due to the vertices and summing over all the site indices of the internal lines. In performing these summations, one cannot sum freely over all the sites of the lattice for each index, since no two lines appearing in a particular intermediate state can be associated with the same site. Furthermore, if the diagram contains equivalent lines, which are defined to be lines of the same type (i.e., dotted, left arrow, right arrow, or more generally, lines having the same indices n and m) that begin at the same vertex and end at the same vertex, then the contribution from the diagram must be divided by a symmetry number, equal to the factorial of the number of equivalent lines. If there is more than one set of equivalent lines, it must be divided by the product

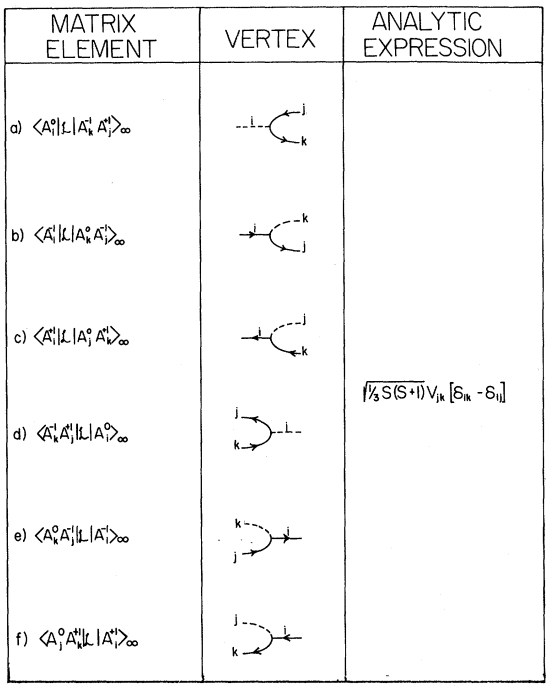

FIG. 1. Basic vertices at $T=\infty$, $S=\frac{1}{2}$.

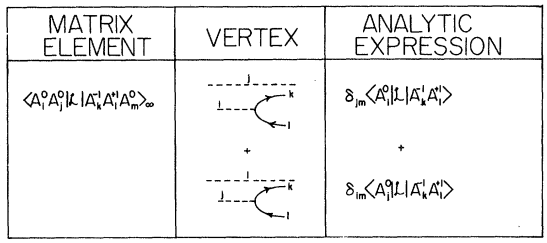

FIG. 2. Example of a general matrix element of $\mathcal{L}$.

of the symmetry numbers for each set. These factors arise because the indices on each line in an intermediate state are summed over independently, so that terms that differ only by a permutation of the indices on a given set of lines all contribute to the sum. However, since all these permutations correspond to the same state, they should only be counted once. Thus each diagram must be divided by a factor giving the number of times the diagram can be taken into itself by permuting the indices of the equivalent lines in an intermediate state. In the present case, there can be no diagrams with equivalent lines. This is not true for general spin or for $T \neq \infty$, except in the particular approximation that we shall describe in Sec. IV. The diagrams contributing to $\langle \omega^2 \rangle_q$ and $\langle \omega^4 \rangle_q$ are shown in Fig. 3. The contribution of Fig. 3(a) is explicitly

$$\tfrac{1}{3}S(S+1) \sum_k \sum_{l \neq k} (V_{kl})^2 (\delta_{il} - \delta_{ik})(\delta_{jl} - \delta_{jk}) = \tfrac{2}{3}S(S+1) \left[\delta_{ij} \sum_k (V_{ik})^2 - V_{ij}^2 \right] \quad (3.3)$$

and hence

$$\langle \omega^2 \rangle_q = \tfrac{2}{3}S(S+1) \left[V^2(0) - V^2(q) \right], \quad (3.4)$$

where $V^2(\vec{q}) = \sum_j e^{-i\vec{q}(\vec{r}_i - \vec{r}_j)} V_{ij}^2$. The restriction in (3.3) on the sums is irrelevant in this case, since $V_{kk} = 0$. However, in the following expression corresponding to Fig 3(c), this restriction does affect the result:

$$\left[\tfrac{1}{3}S(S+1)\right]^2 \sum_{\substack{k,l,0 \\ m \neq l,\ m \neq l}} V_{kl} V_{0l} V_{nm}^2 (\delta_{ik} - \delta_{il})(\delta_{km} - \delta_{kn}) \times (\delta_{0n} - \delta_{0m})(\delta_{j0} - \delta_{jl}) . \quad (3.5)$$

These restrictions are inconvenient, since they prevent the diagrams from being Fourier transformed easily. We shall assume, however, that the interaction V_{ij} is long ranged, so that the number of spins in the range of the interaction, which we denote by c, is large. The range is most easily defined if V_{ij} is a constant for $|\vec{r}_i - \vec{r}_j| \leq R_0$ and 0 otherwise, and we shall assume this to be the case, although we expect our results to hold for more general potentials and any reasonable definition of the range. We denote by c the number of sites in the interaction range. The Weiss limit is defined by the condition that $V_{ij} \to 0$, $c \to \infty$ in such a way that $V(0)$ remains constant. In this limit $V^2(q)$ is $O(1/c)$.

If we ignore the restrictions on the sums appearing in intermediate states, we will make an error that is of order $1/c$ compared to the remainder, since it will effect at most a finite number of terms in a sum containing c terms. Thus, to order $1/c$, the expression for $\langle \omega^4 \rangle_q$ can be obtained from Figs. 3(b)–3(f), with the intermediate states summed freely over all sites. For a simple-cubic or body-centered-cubic lattice, with nearest-neighbor interactions, the contribution to $\langle \omega^4 \rangle_q$ corresponding to Fig. 3(c) is particularly simple, since $V_{ij} V_{jk} V_{ki} \equiv 0$, and is

$$\left[\tfrac{2}{3}S(S+1)\right]^2 V^2(0) \left[V^2(0) - V^2(\vec{q}) \right] .$$

Diagrams with a single dotted line in an intermediate state contribute to $\langle \omega^{2n} \rangle_q$, but not to $\Omega^{2n}(q)$, since the projection operator $I - P$ eliminates precisely these terms. Thus, diagram 3(b), which when Fourier transformed, is equal to $\langle \omega^2 \rangle_q^2$, does not contribute to $\Omega^4(\vec{q})$, which for a simple-cubic or body-centered-cubic lattice is given by

$$\Omega^4(\vec{q}) = \left[\tfrac{2}{3}S(S+1)\right]^2 \left[V^2(0) - V^2(\vec{q}) \right] \times \left\{ 2V^2(0) + \tfrac{1}{2} \left[V^2(0) - V^2(\vec{q}) \right] \right\} . \quad (3.6)$$

The first term in the curly bracket arises from Figs. 3(c) and 3(d), the remainder from Figs. 3(e) and 3(f).

An exact result for $\Omega^4(\vec{q})$ may be obtained by subtracting from (3.6) the contribution from the terms that would have been omitted if the restriction had been honored, which is easily shown to be

$$-12 \left[\tfrac{1}{3}S(S+1)\right]^2 \left[V^4(0) - V^4(q) \right] ,$$

where $V^4(q) = \sum_j e^{-i\vec{q} \cdot (\vec{r}_i - \vec{r}_j)} V_{ij}^4$. Note that $V^4(q) = O(1/c^3)$.

Exact results for the fourth moment at arbitrary spin are readily obtained, but require the introduction of an additional set of vertices shown in Fig. 4.

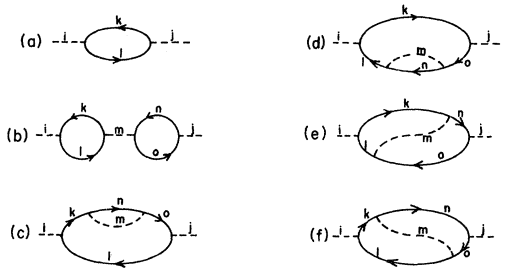

FIG. 3. Diagrams corresponding to second and fourth moment. $\langle A_i^0 | \mathcal{L}^2 | A_j^0 \rangle$ corresponds to (a); $\langle A_i^0 | \mathcal{L}^4 | A_j^0 \rangle$ corresponds to the sum of diagrams (b)–(f).

These contribute to the fourth moment through the diagrams in Fig. 5. We have used double lines to represent the operators A^{2m}. The contribution of Fig. 5(a) is explicitly

$$\frac{C_{20}}{144}\sum_{\substack{k,e,m\\ n,0,p}} V_{nm}{}^2 V_{kl}\, V_{0p}(\delta_{ik}-\delta_{il})(\delta_{jp}-\delta_{j0})(\delta_{kn}\delta_{lm}-\delta_{km}\delta_{ln})(\delta_{pn}\delta_{0m}-\delta_{pm}\delta_{0n}) = \tfrac{2}{5}[\tfrac{1}{3}S(S+1)]^2[4-3/S(S+1)][V^4(0)-V^4(\vec{q})],$$

and the total contribution of all the diagrams in Fig. 5 is

$$[\tfrac{1}{3}S(S+1)]^2[4-3/S(S+1)][V^4(0)-V^4(\vec{q})]\,.$$

The exact fourth moment is the sum of the contribution from the diagrams of Fig. 3, with the restriction respected, together with the contribution from Fig. 5:

$$\omega^4(q) = [\tfrac{2}{3}S(S+1)]^2 \times\Big\{[V^2(0)-V^2(\vec{q})]\{2V^2(0)+\tfrac{3}{2}[V^2(0)-V^2(\vec{q})]\} - [V^4(0)-V^4(\vec{q})]\Big(2+\frac{3}{4S(S+1)}\Big)\Big\}\,. \quad (3.7)$$

This result agrees with that calculated directly from the multiple commutator by Marshall and Lowde.[14]

Note that the contributions to the moments associated with the vertices of Fig. 4 are of the same order in $1/c$ as the error made in omitting the restrictions on the sums corresponding to the diagrams in Fig. 3. This will be true also of higher-order moments and vertices involving A^{nm} with $n>1$, since such vertices occur only when one of the operators that would have been associated with a basic vertex of the type shown in Fig. 1 is on the same site as an operator associated with an on-going line [i.e., in Fig. 3(c) the index n is equal to the index l]. Since any intermediate state will have a finite number of on-going lines, this situation will occur at most a finite number of times in a sum over c sites and hence is negligible as $c\to\infty$. We may, therefore, in calculating the moments to order $1/c$ restrict ourselves to the vertices of Fig. 1.

As a corollary of this observation, we note that $\langle\omega^{2n}\rangle$ must be proportional to $\frac{1}{3}S(S+1)^n$. It follows from (2.11) and the definition of the moments, that the quantity

$$\Sigma^*(\vec{q},z) \equiv [\tfrac{1}{3}S(S+1)]^{1/2}\Sigma(\vec{q},z^*)/\chi(\vec{q},0)\,,$$

where $z^* = z[\frac{1}{3}S(S+1)]^{1/2}$, is independent of spin in the Weiss limit. There exists, therefore, in this limit, a "law of corresponding states" relating the spectral density for different values of spin. This result has some practical significance since it provides a justification for the use of computer calculations on a lattice of classical spins in interpreting data on real three-dimensional systems, where $c\geq 6$ but S is usually $<\frac{7}{2}$.

IV. DIAGRAMMATIC EXPANSIONS AT FINITE TEMPERATURE

The diagrammatic expansions of Sec. III can be extended to finite temperatures if we work in the Weiss limit. The operators we have introduced are not orthonormal at finite temperatures. That is, $\langle A_i^m | A_j^{m'}\rangle = \delta_{ij}\delta_{mm'}$, since the operators on different sites are uncorrelated. The nonorthogonality of the basis at finite temperatures is summarized in the correlation matrix defined by

$$\mathcal{C}\left(\begin{bmatrix}\alpha\\ i\end{bmatrix}_n, \begin{bmatrix}\alpha'\\ i'\end{bmatrix}_{n'}\right) \equiv \beta^{-1}\left\langle A\begin{bmatrix}\alpha\\ i\end{bmatrix}_n \middle| A\begin{bmatrix}\alpha'\\ i'\end{bmatrix}_{n'}\right\rangle\,. \quad (4.1)$$

The symbol $\left[\begin{smallmatrix}\alpha\\ i\end{smallmatrix}\right]_n$ represents a set of indices

$$\begin{Bmatrix}\alpha_1 & \alpha_2 & \cdots & \alpha_n\\ i_1 & i_2 & \cdots & i_n\end{Bmatrix}\,,$$

where the i_j range through the sites of the lattice and the α_j take the values ±1 and 0. The symbol $A\left[\begin{smallmatrix}\alpha\\ i\end{smallmatrix}\right]_n$ denotes the products of the spin operators corresponding to these indices.

The matrix $\mathcal{C}$ corresponds to an operator on V that relates the inner product at $T=\infty$ to the inner product at finite temperatures. That is,

Matrix Element	Vertex	Analytic Expression
$\langle A_i^1 A_j^1 \mid \mathscr{L} \mid A_k^{2,0} A_\lambda^0\rangle_\infty$		$\frac{V_{kl}}{12}\sqrt{\frac{C_{20}}{(1/3)S(S+1)}}\,[\delta_{jl}\delta_{ik}-\delta_{jk}\delta_{il}]$
$\langle A_k^{2,0} A_\lambda^0 \mid \mathscr{L} \mid A_i^1 A_j^1\rangle_\infty$		
$\langle A_i^1 A_j^{-1} \mid \mathscr{L} \mid A_k^{2,-1} A_\lambda^{1}\rangle_\infty$		$\frac{\sqrt{3}V_{kl}}{12}\sqrt{\frac{C_{20}}{(1/3)S(S+1)}}\,[\delta_{jk}\delta_{il}]$
$\langle A_k^{2,-1} A_\lambda^{1} \mid \mathscr{L} \mid A_i^1 A_j^{-1}\rangle_\infty$		
$\langle A_i^1 A_j^1 \mid \mathscr{L} \mid A_k^{2,1} A_\lambda^{1}\rangle_\infty$		$\frac{\sqrt{3}V_{kl}}{12}\sqrt{\frac{C_{20}}{(1/3)S(S+1)}}\,[\delta_{jl}\delta_{ik}]$
$\langle A_k^{2,1} A_\lambda^{1} \mid \mathscr{L} \mid A_i^1 A_j^1\rangle_\infty$		

FIG. 4. Additional vertices contributing to the fourth moment for $S>\frac{1}{2}$.

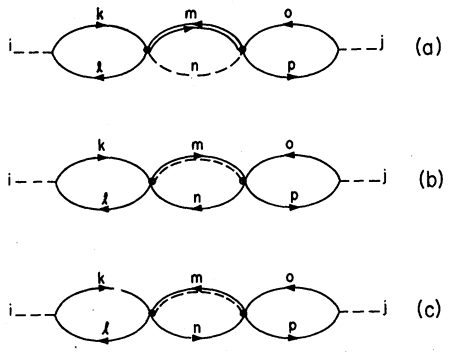

FIG. 5. The total contribution to $\Omega^4(q)$ arising from vertices containing operators with an index $n=2$.

$$\left\langle A\left[\begin{matrix}\alpha\\ i\end{matrix}\right]_n \middle| \mathfrak{C} \middle| A\left[\begin{matrix}\alpha'\\ i'\end{matrix}\right]_{n'} \right\rangle_\infty = \mathfrak{C}\left(\left[\begin{matrix}\alpha\\ i\end{matrix}\right]_n, \left[\begin{matrix}\alpha'\\ i'\end{matrix}\right]_{n'}\right) . \quad (4.2)$$

The operator $\mathfrak{C}$ commutes with $\mathfrak{L}$ since

$$\begin{aligned}\left\langle A\left[\begin{matrix}\alpha\\ i\end{matrix}\right]_n \middle| \mathfrak{L}\mathfrak{C} \middle| A\left[\begin{matrix}\alpha'\\ i'\end{matrix}\right]_{n'} \right\rangle_\infty &= \beta^{-1}\left\langle \mathfrak{L}\times A\left[\begin{matrix}\alpha\\ i\end{matrix}\right]_n \middle| A\left[\begin{matrix}\alpha'\\ i'\end{matrix}\right]_{n'} \right\rangle \\ &= \beta^{-1}\left\langle A\left[\begin{matrix}\alpha\\ i\end{matrix}\right]_n \middle| \mathfrak{L}\times A\left[\begin{matrix}\alpha'\\ i'\end{matrix}\right]_{n'} \right\rangle \\ &= \left\langle A\left[\begin{matrix}\alpha\\ i\end{matrix}\right]_n \middle| \mathfrak{C}\mathfrak{L} \middle| \mathfrak{a}\left[\begin{matrix}\alpha'\\ i'\end{matrix}\right]_{n'} \right\rangle_\infty . \end{aligned} \quad (4.3)$$

The moments can be expressed as

$$\langle \omega^{2n} \rangle_q = \frac{\beta \langle A^0(q) | \mathfrak{L}^{2n} \mathfrak{C} | A^0(q) \rangle_\infty}{\langle A^0(q) | A^0(q) \rangle} \quad (4.4)$$

or upon inserting a complete set of states,

$$\langle \omega^{2n} \rangle_q = \beta \sum_{k=1}^{\infty} \frac{1}{k!} \sum_{\left[\begin{matrix}\alpha\\ i\end{matrix}\right]_k}{}' \left\langle A^0(q) \middle| \mathfrak{L}^{2n} \middle| A\left[\begin{matrix}\alpha\\ i\end{matrix}\right]_k \right\rangle_\infty \times \left\langle A\left[\begin{matrix}\alpha\\ i\end{matrix}\right]_k \middle| \mathfrak{C} \middle| A^0(q) \right\rangle_\infty \Big/ \langle A^0(q) | A^0(q) \rangle . \quad (4.5)$$

The symbol $\sum'_{\left[\begin{matrix}\alpha\\ i\end{matrix}\right]_k}$ indicates that each index in the set $\left[\begin{matrix}\alpha\\ i\end{matrix}\right]$ is to be summed over its entire range independently of the other indices, with the exclusion of any two or more indices on the same site.

From the fluctuation dissipation theorem and the fact that the moments are all at least $O(1/c)$, it is easy to see that

$$\left\langle A\left[\begin{matrix}\alpha\\ i\end{matrix}\right]_n \middle| A\left[\begin{matrix}\alpha'\\ i'\end{matrix}\right]_m \right\rangle = \beta \left\langle\left\langle A\left[\begin{matrix}\alpha\\ i\end{matrix}\right]_n^\dagger A\left[\begin{matrix}\alpha'\\ i'\end{matrix}\right]_m \right\rangle\right\rangle \times [1+O(1/c)] .$$

Thus the matrix elements of $\mathfrak{C}$ can all be calculated from the equilibrium correlation functions. We can define the cumulant averages, of a set of operators $\left[\begin{matrix}\alpha\\ i\end{matrix}\right]_n$, which we denote by $K\left[\begin{matrix}\alpha\\ i\end{matrix}\right]_n$, recursively by means of the definition

$$\left\langle\left\langle A\left[\begin{matrix}\alpha\\ i\end{matrix}\right]_n \right\rangle\right\rangle = \sum_{\{m_l\}} \sum_P \left\{K\left[\begin{matrix}\alpha_P\\ i_P\end{matrix}\right]_1 \cdots K\left[\begin{matrix}\alpha_P\\ i_P\end{matrix}\right]_1\right\}\left\{K\left[\begin{matrix}\alpha_P\\ i_P\end{matrix}\right]_2 \cdots\right\} \cdots K\left[\left[\begin{matrix}\alpha_P\\ i_P\end{matrix}\right]_n . \quad (4.6)$$

(m_1 factors; m_2 factors; m_n factors)

The first sum is over all sets of integers such that

$$\sum_{l=1}^{n} l m_l = n ,$$

and the sum over permutations is the sum over all of the distinct ways in which the indices $\left[\begin{matrix}\alpha\\ i\end{matrix}\right]_n$ can be distributed into the sets forming the arguments of the K's. Clearly, the matrix elements can all be expressed in terms of $K\left[\begin{matrix}\alpha\\ i\end{matrix}\right]_n$ with $n \geq 2$. We represent

$$\mathfrak{C}\left(\left[\begin{matrix}\alpha\\ i\end{matrix}\right]_n, \left[\begin{matrix}\alpha'\\ i'\end{matrix}\right]_{n'}\right)$$

graphically as a vertical line with n horizontal lines attached to it on the left, and n' lines attached on the right. The cumulant averages will be denoted by wavy lines linking the various horizontal lines, where the number of wavy lines will be one less than the index of the cumulant average. The wavy lines are intended to indicate the order of magnitude of the cumulants in $1/c$, which may be estimated using the diagrammatic expansion of the equilibrium averages introduced by Stinchcombe *et al.*[15] Each line represents a power of $1/c$ (see Fig. 6). The matrix element $\langle A_i^0 | \mathfrak{L}^{2n} | A\left[\begin{matrix}\alpha\\ i\end{matrix}\right]_k \rangle_\infty$ is equal to the sum of all infinite-temperature diagrams beginning on the left with a dotted line and ending on the right with k lines of the type determined by the set α. The matrix elements

$$\mathfrak{C}\left(\left[\begin{matrix}\alpha\\ i\end{matrix}\right]_k ; \left[\begin{matrix}0\\ i\end{matrix}\right]_1\right)$$

connect these with wavy lines along the vertical line. A typical graph is shown in Fig. 7. We note

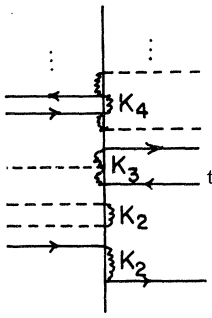

FIG. 6. Diagrammatic representations of the equilibrium correlations.

that the contribution from the term for which $k=1$ in Eq. (4.5) is simply the infinite-temperature result. An expansion in β can be obtained by keeping a finite number of terms in the sum over k in (4.5), and expanding the correlation functions in powers of β.

We wish to keep only those terms in the sum (4.5) that are of the same order in $1/c$ as the infinite-temperature value of the moments. This can be accomplished by simply neglecting all the cumulants K_n with $n>2$. To see why this is so, consider the graph for $\langle\omega^4\rangle_a$ shown in Fig. 8, involving a K_3 term.

The intermediate lines have been labeled with indices corresponding to a particular choice of the δ functions appearing in the vertices, so that the contribution corresponding to the diagram in Fig. 8 is only part of the total contribution from the diagram with the structure of Fig. 8 but composed of vertices in which both lines entering or leaving a vertex have free indices. We shall call a diagram in which the δ functions have been eliminated a reduced part. The order of magnitude, in $1/c$, of the reduced part may be estimated most easily by inspections of the dual of the graph composed of the dynamical vertices, which is obtained by replacing the vertices by lines and the lines by points. The lines arising from the correlations are left as lines.

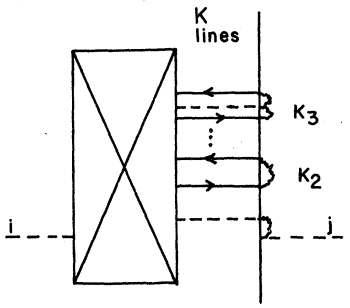

FIG. 7. A contribution to $\langle A_i^0|\mathfrak{L}^{2m}|A_j^0\rangle$, for which $k=n$ in the sum (4.5). The block denotes a matrix element $\langle A_i^0|\mathfrak{L}^{2m}|A[{}^{\alpha}_{k}]_n\rangle_\infty$.

In the combined graphs, Fig. 8(b), all the lines, whether they arise from the correlations or the dynamical vertices, are of order $1/c$. The order of magnitude of the graph is simply $1/c$ to a power equal to the difference between the number of lines and the number of free summations, in this case $(1/c)^4$, which is a factor of $1/c$ smaller than the high-temperature graph for which $i\neq n$. Note that the summation over the index k in Fig. 8 leaves the order of magnitude of the graph unchanged, whereas a summation over a vertex with three or more lines will lower the order of the graph by at least a factor of $1/c$. Since the only terms arising from the correlations that can lead to vertices in the combined graph at which only two lines enter are those arising from K_2, only those terms need be considered.

The approximation of $\mathfrak{C}$ by the terms involving only K_2 allows a great simplification of the problem of calculating the moments. Furthermore, the restriction on $\mathfrak{C}$ arising from the fact that it must commute with $\mathfrak{L}$ is actually sufficient to determine K_2 uniquely! Consider the graphical expansion of the identity

$$\left\langle A\left[{}^{\alpha}_{i}\right]_k \middle| \mathfrak{L}\,\mathfrak{C} - \mathfrak{C}\,\mathfrak{L} \middle| A\left[{}^{\alpha'}_{i'}\right]_{l'} \right\rangle_\infty = 0 \tag{4.7}$$

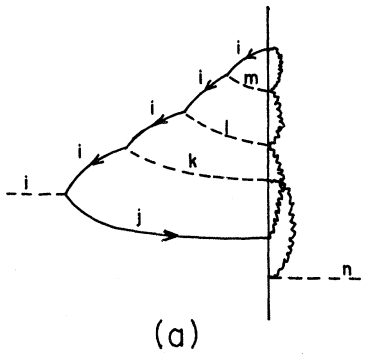

(a)

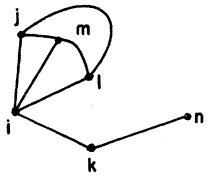

(b)

FIG. 8. A temperature-dependent contribution to $\langle A_i^0|\mathfrak{L}^4|A_n^0\rangle$ involving a cumulant average k_3. The graph in (b) is dual of that in (a), in which the dynamical vertices have been replaced by lines, and the solid or dotted lines by points. The contribution of this graph is a factor of $1/c$ smaller than the infinite-temperature matrix elements.

first for the case that the set $[{}^{\alpha'}_{i'}]_l$ is null, and then for the general case. Since $\mathcal{L}|A^{00}\rangle\equiv 0$, (4.7) reduces to

$$\sum_l \sum_{[{}^{\alpha'}_{i'}]_l} \frac{1}{l!}\left\langle A\left[{}^{\alpha}_{i}\right]_k \middle| \mathcal{L} \middle| A\left[{}^{\alpha'}_{i'}\right]_l \right\rangle_\infty e\left(\left[{}^{\alpha'}_{i'}\right]_l, [0]\right) = 0 \,. \tag{4.8}$$

A typical term in the graphical expansion corresponding to (4.8) is shown in Fig. 9. For fixed indices i, j, k, this diagram must be summed over the index l. There are, however, five other diagrams that also can contribute for the same values of i, j, k. These are obtained by replacing the diagram in the dotted box of Fig. 9(a) by the diagrams 9(b)–9(f). In order for (4.8) to hold, we must have that the sum of the contributions from these diagrams is zero. In performing the summation over the diagrams 9(e) and 9(f), one must omit the terms for which the summation indices l or m are equal to other indices appearing on the vertical line, since these terms are not contained in (4.8). Let us denote the wavy line which represents $\langle\langle A^0_i A^0_j\rangle\rangle$ by $\rho(i-j)$. If $i=j$, $\rho(0)=1$. If we lift the restrictions on the sums in the diagrams 9(d)–9(f), then the additional terms that are added by lifting the restriction are equal, to order $1/c$, to the contribution from the diagrams 9(a)–9(c). For instance, the term for which $l=j$ in diagram 9(d) and the term for which $l=i$ in diagram 9(f) combine to give

$$[\tfrac{1}{3}S(S+1)]^{1/2}\sum_m V_{ij}(\delta_{mj}-\delta_{mi})\rho(m-k) \,,$$

which is precisely the contribution of Fig 9(c). The terms that are added, in which both indices l, m in Figs. 9(d)–9(f) are equal to the index to which they are connected by a wavy line, combine to give no contribution. There are terms that do not cancel identically, resulting from the indices l, m being equal to one of the indices in $[{}^{\alpha}_{i}]_k$ to which they are not connected by a wavy line [$l=k$ in diagram 9(d), for instance]. These, however, are at least $O(1/c^3)$, which is at least one factor of $1/c$ smaller than the total contribution of the diagrams, and may be neglected. Thus, the contribution from all the diagrams 7(a)–7(c) is given, to lowest order in $1/c$, by

$$\begin{aligned}[\tfrac{1}{3}S(S+1)]^{1/2}\sum_l\sum_m V_{lm}[&(\delta_{il}-\delta_{im})\rho(l-j)\rho(m-k)\\ &+(\delta_{kl}-\delta_{km})\rho(l-i)\rho(m-j)\\ &+(\delta_{jm}-\delta_{jl})\rho(l-i)\rho(m-k)] \,.\end{aligned} \tag{4.9}$$

In order to satisfy (4.8), (4.9) must be zero for all i, j, k such that $i\neq j\neq k$. However, it is easily seen that (4.9) vanishes whenever any two indices are equal, so with no loss of generality, we can require that (4.9) vanish for all values of the indices i, j, k. This is equivalent to the following equation for

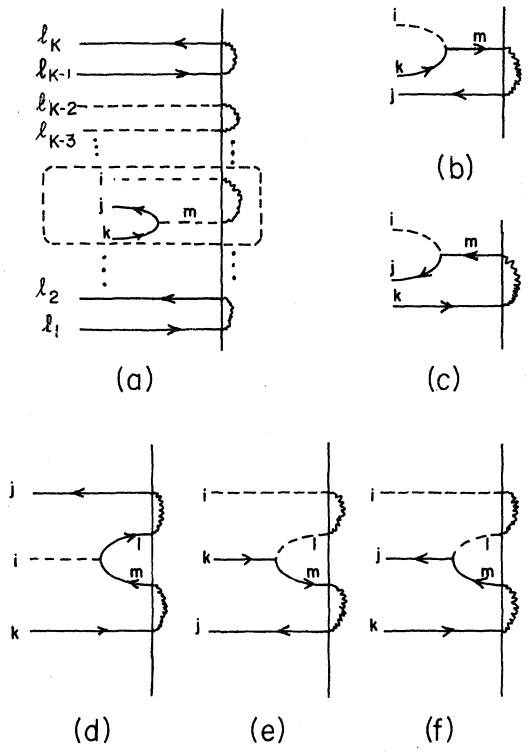

FIG. 9. (a) A general term in the graphical expansion of (4.24). The section of the diagram in the dotted box can be replaced by any of the diagrams (b)–(f). The complete matrix element is the sum of all six diagrams formed in this way.

all $\vec{q}_1$, $\vec{q}_2$, $\vec{q}_3$ such that $\vec{q}_1+\vec{q}_2+\vec{q}_3=0$:

$$\begin{aligned}[V(\vec{q}_1)-V(\vec{q}_2)]\rho(\vec{q}_1)\rho(\vec{q}_2)+[V(\vec{q}_2)-V(\vec{q}_3)]\rho(\vec{q}_2)\rho(\vec{q}_3)\\ +[V(\vec{q}_3)-V(\vec{q}_1)]\rho(\vec{q}_1)\rho(\vec{q}_3)=0 \,.\end{aligned} \tag{4.10}$$

We observe that if $\rho(\vec{q})$ is of the form

$$\rho(\vec{q})=[\alpha_1+\alpha_2 V(\vec{q})]^{-1} \,, \tag{4.11}$$

then (4.10) will be identically satisfied since we will have

$$\rho(\vec{q}_1)-\rho(\vec{q}_2)=\alpha_2[V(\vec{q}_2)-V(\vec{q}_1)]\rho(\vec{q}_2)\rho(\vec{q}_1) \,. \tag{4.12}$$

Equation (4.12), together with the condition

$$N^{-1}\textstyle\sum_q \rho(q)=1 \,, \tag{4.13}$$

which was used in the derivation of (4.10), specifies a one-parameter family of equilibrium correlation functions.

Let us consider Eq. (4.7) for arbitrary states $[{}^{\alpha}_{i}]_k$ and $[{}^{\alpha'}_{i'}]_l=[{}^{0}_{i}]_1$. We will have then, instead of (4.8), the analogous expression with [0] replaced by $[{}^{0}_{i}]_1$. A typical term in the matrix element $\langle A[{}^{\alpha}_{i}]_k|\mathcal{L}e|A^0_i\rangle_\infty$ may be represented by the diagram of Fig. 10(a). A contribution to the same matrix

element of $\mathcal{C}\mathcal{L}$ is shown in Fig. 10(b). According to (4.7), when diagrams of the type 10(a) are summed over all intermediate states, the result is 10(b). The matrix element of $\mathcal{L}$ appearing in 10(a) contains one elementary vertex, so that the number of lines appearing in the intermediate state is either $k+1$ or $k-1$. Unless one of the lines of that vertex is connected to the dotted line at the site i, the matrix element vanishes, by the result just demonstrated. The only diagrams possible, therefore, are shown in Figs. 10(c)–10(e). Thus, diagram 10(b) must be equal to the sum of diagrams 10(c)–10(e). We observe that the correlations involving lines entering from different sides of the vertical line include the term for which the two indices are identical, since they correspond to different states, and that omitting the restrictions on the index l in diagrams 10(d) and 10(e) includes diagram 10(c). We have, therefore, that the following will hold if (4.7) does:

$$[\tfrac{1}{3}S(S+1)]^{1/2}\textstyle\sum_l\sum_m V_{lm}(\delta_{im}-\delta_{il})\rho(l-K)\rho(m-j)=[\tfrac{1}{3}S(S+1)]^{1/2}\sum_l\sum_m V_{lm}[(\delta_{Km}-\delta_{Kl})\rho(l-j)\rho(i-m)$$
$$+(\delta_{jl}-\delta_{jm})\rho(l-K)\rho(i-m)]\,. \qquad (4.14)$$

This need only hold for $j\neq k$, but again is valid for $j=k$, and hence is equivalent to the requirement that the following will hold for all $\vec{q}_1$, $\vec{q}_2$:

$$N^{-1/2}[\tfrac{1}{3}S(S+1)]^{1/2}[V(\vec{q}_1)-V(\vec{q}_2)]\rho(\vec{q}_2)\rho(\vec{q}_1)=N^{-1/2}[\tfrac{1}{3}S(S+1)]^{1/2}\{[V(\vec{q}_1)-V(\vec{q}_1+\vec{q}_2)]\rho(\vec{q}_1+\vec{q}_2)\rho(\vec{q}_1)$$
$$+[V(\vec{q}_1+\vec{q}_2)-V(\vec{q}_2)]\rho(\vec{q}_1+\vec{q}_2)\rho(\vec{q}_2)\}\,. \qquad (4.15)$$

Equation (4.15) is identical to the condition (4.10), and places no further restrictions on $\rho(q)$. The parameter α_2 can be identified by using the exact relation

$$\langle A^{+1}(\vec{q}_1)A(\vec{q}_2)^{-1}\,|\,\mathcal{C}\mathcal{L}\,|\,A^0(\vec{q}_1+\vec{q}_2)\rangle_\infty=\beta^{-1}\langle A^+(\vec{q}_1)A^-(\vec{q}_2)\,|\,\mathcal{L}\,|\,A^0(\vec{q}_1+\vec{q}_2)\rangle$$
$$=\beta^{-1}\langle\langle[A^0(\vec{q}_1+\vec{q}_2),\,A^{+1}(-\vec{q}_2)A^{-1}(-\vec{q}_1)]\rangle\rangle$$
$$=\{\beta[\tfrac{1}{3}S(S+1)]^{1/2}\}^{-1}N^{-1/2}[\rho(\vec{q}_1)-\rho(\vec{q}_2)]. \qquad (4.16)$$

The term on the left of (4.15) is precisely the matrix element in (4.16) calculated diagrammatically. Using (4.12) we have therefore that $\alpha_2=-\beta\frac{1}{3}[S(S+1]$. α_1 can be evaluated from the identity

$$\rho(q)\big|_{q=0}=[\beta\tfrac{1}{3}S(S+1)]^{-1}\chi(0,0)=[\alpha_1+\alpha_2V(0)]^{-1}\,. \qquad (4.17)$$

Hence, (4.11) becomes

$$\rho(q)=[\beta\tfrac{1}{3}S(S+1)]^{-1}\,\frac{1}{1/\chi+V(0)-V(q)}\,, \qquad (4.18)$$

where $\chi=\chi(0,0)$.

The correlation function (4.18), together with the condition (4.13), completely specifies the spherical model solution for $\rho(q)$, which has been shown by Brout,[16] on the basis of a diagrammatic analysis of the correlation functions in the canonical ensemble, to be asymptotically correct in the limit $c\to\infty$. We emphasize that it has been derived here from the dynamical condition (4.5), evaluated in the limit $c\to\infty$, assuming that the cumulant functions K_n, $n>2$, were higher order in $1/c$ than K_2, and that K_2 was of order $1/c$. It is surprising that such weak assumptions should lead to such a strong result, but there are well-known precedents for this. The nonlinear Boltzmann equation, which can be derived from the exact dynamics as an asymptotic expansion in the density, has as an equilibrium solution a two-parameter family of distributions that can be identified with the Fermi-Dirac or Bose-Einstein distributions when the parameters are related to the chemical potential and the temperature. The close parallel of that result with the present diagrammatic derivation will be evident in a subsequent paper, where (4.10) and (4.15) are rederived using kinetic equations.

Equation (4.18) has also been derived[17,18] on the basis of what has been called "the random-phase approximation" (RPA) and the fluctuation dissipation theorem. The RPA can be justified as being exact in the limit[19,20] $c\to\infty$ in the presence of a spontaneous magnetization, so that it is not unexpected that (4.18) can be derived using it. The derivation has a serious inconsistency, however, in that it assumes that all dynamical correlations vanish in order to calculate the equilibrium correlations. The present derivation is more satisfactory, in that it assumes only an order of magnitude for the equilibrium correlation function, in order to calculate it.

Resibois and DeLeneer have derived results whose physical content appears to be identical with the implication of (4.10), namely, that the

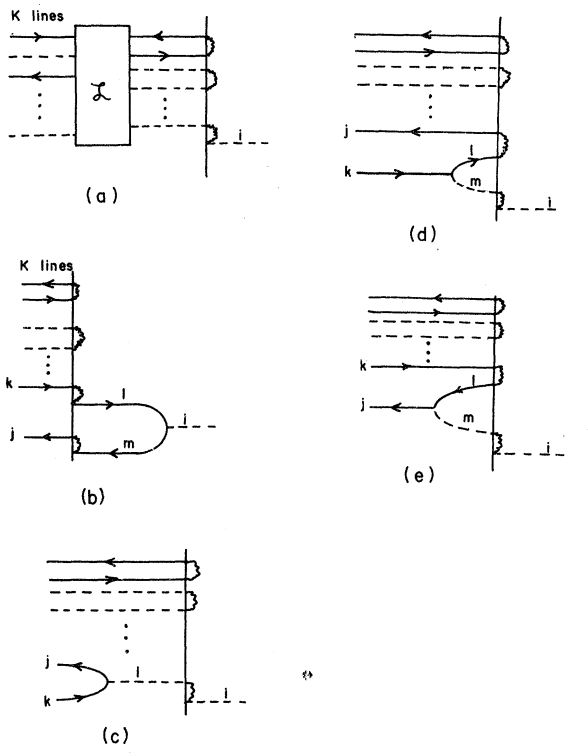

FIG. 10. (a) A general matrix element $\langle A[^{\alpha}_{i}]_k | \mathfrak{L}\mathfrak{C} | A^0_{\nu}\rangle_\infty$; (b) general matrix element $\langle A[^{\alpha}_{i}]_k | \mathfrak{C}\mathfrak{L} | A^0_i\rangle_\infty$; (c)–(f) the only nonvanishing diagrams corresponding to (a). The sum of the diagrams (c)–(f) is equal to the diagram (b).

Liouville operator when calculated to lowest order in $1/c$ propagates unchanged the equilibrium correlations that are lowest order in $1/c$. There does not appear to be any relation in their theory similar to (4.15) and (4.16) that would restrict the equilibrium correlation function to the spherical model, and indeed, they use for $\rho(q)$ the expression

$$\rho(q) = [1 - \beta\tfrac{1}{3}S(S+1)V(q)]^{-1} , \qquad (4.19)$$

which is less accurate than (4.18), and does not satisfy (4.13).

The equivalence of diagram 10(b) with the sum of diagrams 10(c)–10(e) allows one to eliminate the equilibrium correlation matrix $\mathfrak{C}$ from the diagram entirely, in favor of a temperature-dependent vertex function. Consider, for instance, the diagrams representing the nonzero matrix elements of

$$\left\langle A\left[{}^{\alpha}_{i}\right]_K \middle| \mathfrak{L}^2\mathfrak{C} \middle| A\left[{}^{0}_{i}\right]_1 \right\rangle_\infty .$$

From the results above, these can only be of the types shown in Figs. 11(a)–11(d), and furthermore, diagrams 11(a)–11(c) can be combined to give Fig. 11(e). In order to cast Fig. 11(d) in the same form as Fig. 11(e), that is, with the matrix elements of the correlation operator on the left, we define the function

$$\rho^{-1}(i-j) \equiv N^{-1}\textstyle\sum_q e^{i\vec{q}\cdot(\vec{r}_i-\vec{r}_j)}[\rho(q)]^{-1} , \qquad (4.20)$$

which satisfies

$$\textstyle\sum_m \rho^{-1}(i-m)\rho(m-j) = \delta(i-j) . \qquad (4.21)$$

We will represent this function by an x appearing on a line (i.e., $\overset{i}{\text{---}}\text{x}\text{---}\overset{j}{}$). Then 11(d) can be written as 11(f), with the matrix elements of C appearing to the left. We observe that the two diagrams 11(a) and 11(d) are the only ones that exist in the high-temperature limit, and that the section of the diagram to the right of the vertical line in 11(e) is precisely the high-temperature limit of 11(a). By moving the line representing the correlation matrix elements to the left, one sees that the effect of the correlations is simply to replace all the left vertices in the infinite-temperature diagrams by renormalized vertices, the renormalized vertex representing the diagram and analytical expression corresponding to the section of diagram 11(f) that is enclosed in the dotted box, and to replace the initial dotted line at site i by $\rho(i-i')$. The analytic expression corresponding to a par-

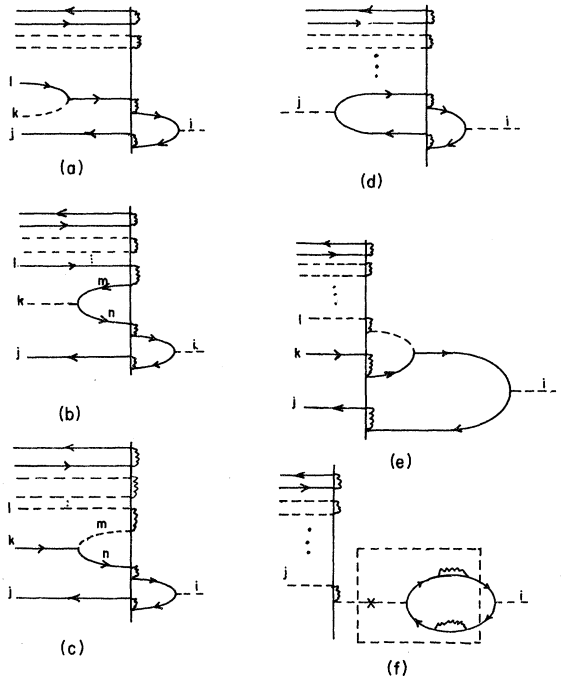

FIG. 11. (a)–(d) The nonvanishing diagrams corresponding to $\langle A[^{\alpha}_{i}]_k | \mathfrak{L}^2\mathfrak{C} | A[^{0}_{i}]_1\rangle_\infty$; (a)–(c) combine to yield (e); (d) and (f) are equivalent diagrams. The effect of the equilibrium correlations in an arbitrary diagram is the replacement of the left vertices by the renormalized vertex shown in the dotted box in (f).

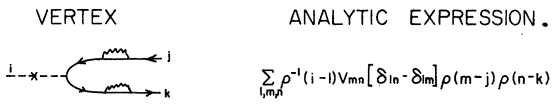

FIG. 12. The diagrams for a renormalized vertex and its analytic expression.

ticular renormalized vertex is given in Fig. 12. Since it is clear that there is no antisymmetry in the theory between right and left (the line representing the correlations could have been started on the left and moved to the right), one could as well replace left vertex by right vertex in the above paragraph, and initial line by final line. Indeed, the results we have derived have their simplest physical interpretation if one renormalizes both vertices. Since there are no restrictions on the summations, the diagrams can most conveniently be expressed directly in the Fourier-transformed variable. We summarize the above results in a set of rules for calculating the moments with both vertices renormalized.

Rules for Calculation of $\langle \omega^{2n} \rangle_q$

(1) Draw all distinct graphs beginning on the left and ending on the right with a dotted line that can be constructed from $2n$ of the basic vertices. Two graphs that differ in the sequence, from left to right, that the vertices occur are considered distinct.

(2) Label the initial and final lines with the momentum index $\vec{q}$. Label all internal lines with indices $\vec{q}_i$.

(3) Associate with each vertex the appropriate analytic expression, taken from Fig. 13, and take their product.

(4) Sum over all indices $\vec{q}_i$.

The rules as we have outlined them are precisely what one would obtain if one regards the set of operators

$$\prod_{[q_i^{\alpha}]_n} \rho(\vec{q}_i)^{-1/2} A\begin{bmatrix} \alpha \\ \vec{q} \end{bmatrix}_n \equiv \tilde{A}\begin{bmatrix} \alpha \\ q \end{bmatrix}_n$$

as an orthonormal set in the inner product $\langle A|B\rangle_\beta = \beta^{-1}\langle A|B\rangle$. That is, we write the identity operator as

$$I = |A^{00}\rangle\langle A^{00}| + \sum_q \sum_{i=-1}{}' |A^{\alpha i}(\vec{q})\rangle\langle A^{\alpha i}(\vec{q})|\rho(\vec{q})^{-1}$$

$$+ \frac{1}{2!}\sum_{q_1}\sum_{q_2}\sum_{i=-1}^{i=+1}\sum_{i'=-1}^{i'=+1} |A^{\alpha i}(\vec{q}_1)A^{\alpha i'}(\vec{q}_2)\rangle$$

$$\times\langle A^{\alpha i}(\vec{q}_1)A^{\alpha i'}(\vec{q}_2)|\rho(\vec{q}_1)^{-1}\rho(\vec{q}_2)^{-1} + \cdots, \quad (4.22)$$

and then insert this expression for the identity operator between powers of $\mathcal{L}$ in the definition (4.6). In calculating the matrix elements, we would then assume that the following is true:

$$\beta^{-1}\prod_{[q_i^{\alpha i}]_n} \rho(\vec{q}_i)^{-1}\left\langle A\begin{bmatrix}\alpha_i \\ q_i\end{bmatrix} \middle| A\begin{bmatrix}\alpha_{i'} \\ q_{i'}\end{bmatrix}\right\rangle = \delta\left(\begin{bmatrix}\alpha_i \\ q_i\end{bmatrix}, \begin{bmatrix}\alpha_i' \\ q_i'\end{bmatrix}\right). \quad (4.23)$$

In fact, of course, (4.23) is not correct, even if we calculate the matrix elements to lowest order in $1/c$. For instance, $\langle A^0(q)A^0(-q)|A^{00}\rangle \neq 0$. What we have shown, however, is that the terms coming from the nonorthogonality of the $\tilde{A}[q_i^{\alpha i}]$ cancel, to order $1/c$, in calculating the moments, so that one may simply regard (4.22) and (4.23) as valid in an operational sense.

The states $|\tilde{A}[q_i^{\alpha}]_n\rangle$ can be thought of as representing a state of the system in which n independent fluctuations of wave vector $q_1 \cdots q_n$ are superimposed on the thermal equilibrium background. The sole effect of the presence of correlations in equilibrium, in the present approximation, is to change the rate at which these modes decay into one another, as given by the matrix elements of $\mathcal{L}$. From the analytic expressions accompanying Fig. 11, it is clear that the correlations act to enhance the probability of a decay into those fluctuations for which $\rho(q)$ is largest, i.e., the critical fluctuations.

Using these rules, we have for the second moment the expression

$$\langle \omega^2 \rangle_q = \tfrac{1}{3}S(S+1)N^{-1}\sum_{q'} [V(q') - V(q-q')]^2 \rho(q')\rho(q-q')\rho(q)^{-1}. \quad (4.24)$$

The expression for $\Omega^4(q)$ is

$$\Omega^4(q) = \tfrac{2}{3}S(S+1)N^{-1}\sum_{q'} [V(q-q') - V(q')]^2 \langle \omega^2 \rangle_{q'} \rho(q')\rho(q-q')\rho(q)^{-1}$$
$$+ 2[\tfrac{1}{3}S(S+1)]^2 N^{-2}\sum_{q'}\sum_{q''} [V(q-q') - V(q')][V(q'') - V(q-q'-q'')]$$
$$\times [V(q'+q'') - V(q-q'-q'')][V(q'') - V(q')]\rho(q')\rho(q'')\rho(q-q'-q'')\rho(q)^{-1}. \quad (4.25)$$

The integral in (4.24) can be calculated explicitly for the simple-cubic lattice with nearest-neighbor interactions and is

$$\langle \omega^2 \rangle_q = 12\Theta^{-2}[(1/\chi|V(0)| + 1)\Theta - 1]$$
$$\times [V^2(0) - V^2(\vec{q})]\rho(\vec{q})^{-1}. \quad (4.26)$$

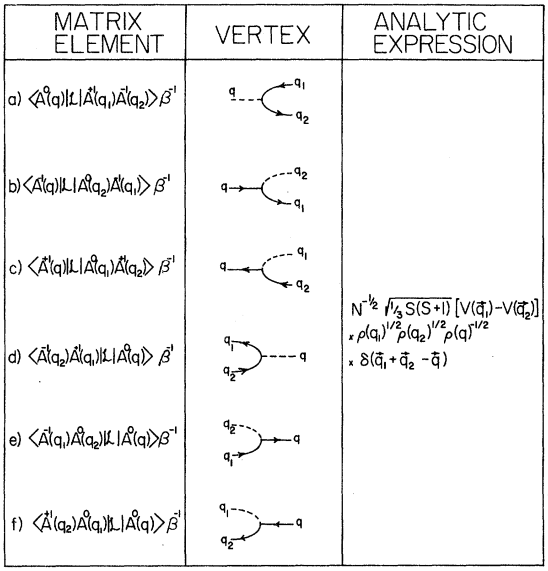

FIG. 13. The basic renormalized vertices in the momentum representation.

The formula holds for both the ferromagnet and the antiferromagnet, with χ replaced by the staggered susceptibility for the antiferromagnet. Θ is defined as $|V(0)|\beta\frac{1}{3}S(S+1)$.

The diagrams we have constructed are superficially similar to those used by Resibois and DeLeneer, but the rules for calculation are significantly different. Resibois and DeLeneer have used basis states, which they denote by $|\{u\}\rangle$, that do not span V. As a result, a matrix "element" of $\mathcal{L}$, in their terminology, is an operator on V, and the diagrams represent sequences of operators. We see no advantage in this procedure, as their rules of calculation are significantly more complicated than the ones we present. Furthermore, by separating the Liouville operator into a transverse and longitudinal part, they introduce additional vertices, those with two "semiconnection bonds," not present in our theory. This separation is clearly artificial in the paramagnetic regime. A further objection is the limitation of the theory to $S=\frac{1}{2}$, which obscures the simple dependence of the moments on the spin in the Weiss limit. The diagrammatic method developed by Wegner differs from the one we have described in the definition of the inner product at finite temperatures and the treatment of the operators Y^{nm} with $n>1$, at all temperatures. An effect of the former difference is to introduce a vertex that does not involve any change in the number of modes, which is not present in our theory, and which vanishes at infinite temperatures. The latter difference obscures the simplicity of the Weiss limit.

V. RESUMMATION OF DIAGRAMS

The moment expansion (2.12) when carried out to any finite number of terms allows one to approximate the relaxation function $\Sigma(q,t)$ by a polynomial in t. Such an approximation is valid only for times sufficiently short that one can neglect the remainder of the terms in the series. If one wants expressions for $\Sigma(q,t)$ valid for arbitrary times, it is necessary to sum an infinite number of terms in the moment expansion. One of the virtues of the diagrammatic method of calculating the moments is that it enables one to do this readily. Unfortunately there is no small parameter in the problem with which to select some subset of the diagrams and assert that it is the dominant contribution. The parameter c will not do since all the diagrams contributing to $\langle\omega^{2n}\rangle_q$ are proportional to c^{-n}. The criterion for the success of any resummation procedure must therefore rest upon a comparison of the results for $\Sigma(q,t)$ with experiment, and the derivation will need to appeal to intuitive notions about the relative significance of the physical processes corresponding to different sequences of diagrams.

The most straightforward resummation consists of combining all those diagrams that differ only in the sequence, from left to right, that the vertices appear. This may be accomplished by choosing one such diagram, and assigning to each vertex a time t_i with the vertex t_{i+1} to the right of t_i. Since

$$\int_0^t dt_1 \cdots \int_{t_{n-1}}^t dt_n = t^n/n!\ ,$$

the correct time-dependent factor associated with the diagram is obtained by integrating over all times in the region $0<t_1<\cdots t_n<t$, i.e., by integrating over that wedge of the hypercube for which the sequence of the vertices is unchanged as the t_i vary. If we leave the labels affixed to the vertices, and consider a diagram that differs only in the sequence in which the vertices occur, it will correspond to integrating over a different wedge of the hypercube. Since exchanging the relative positions of two vertices leaves a diagram unchanged if and only if they are not connected by a line, we can account for all the possible time orderings of a particular diagram by introducing a factor $\Theta(t_f-t_i)$ for each line joining a vertex at t_i

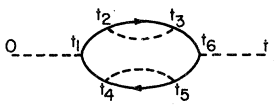

FIG. 14. Time labeled diagram contributing to the sixth moment. The diagram includes the contribution from the six time-independent diagrams differing in the order of the vertices labeled t_2-t_5.

to one at t_f, and integrating over the full hypercube. Having made the association of the factor $\Theta(t_f - t_i)$ with each line, we then regard all diagrams that differ only in their time ordering as equivalent. For instance, the diagram of Fig. 14 contributes a time-dependent factor

$$\int_0^t dt_6 \int_0^{t_6} dt_1 \int_{t_i}^{t_6} dt_4 \int_{t_1}^{t_6} \int dt_2 \int_{t_2}^{t_6} dt_3 \int_{t_4}^{t_6} dt_4 = 6\,\frac{t^6}{6!}$$

and corresponds to the $4!/2!2! = 6$ time-independent diagrams that are obtained by permuting the order in which the vertices labeled t_2 and t_3 occur with respect to those labeled t_4 and t_5. A further resummation can now be obtained in the manner described by Resibois and DeLeneer and by Wegner. A diagonal subdiagram is defined as a section of a diagram that begins and ends with the same line. A general diagram can be reduced to its skeleton by removing all diagonal subdiagrams, and a diagram that corresponds to its skeleton is said to be irreducible. The entire set of diagrams may be obtained by inserting, for each line of all the irreducible diagrams, all possible diagonal subdiagrams. The sum of all possible diagonal subdiagrams corresponding to a line labeled with the index q is just $\Sigma(q,t)/\chi(q,0)$. Hence we have the result that the entire series is obtained by (1) constructing all possible irreducible diagrams using the vertices of Fig. 13, (2) assigning a time label to each vertex and multiplying the contribution from the vertices by a factor of $\Theta(t_f - t_i)\Sigma(q_i, t_j - t_i)/\chi(q_i, 0)$ for each line labeled by q_i between the vertices at time t_i and t_f, and (3) multiplying by $(-1)^n$, where $2n$ is the number of vertices, integrating over all intermediate times and summing over all intermediate momenta.

Approximations to this series are obtained by summing only a finite number of the irreducible diagrams. The approximate equations of Kawasaki, of Resibois and DeLeneer,[11] of Wegner,[12] and of Blume and Hubbard[21] all correspond to using the simplest irreducible diagram, Fig. 3(a). In a subsequent paper, we will discuss an alternative resummation procedure that makes use of a set of kinetic equations and leads to self-consistent equations for the vertex function, rather than the propagator.

---

*Research supported in part by the Air Force Office of Scientific Research, Office of Aerospace Research, USAF under AFOSR Grant No. 68-1448.

[1]B. I. Halperin and P. C. Hohenberg, Phys. Rev. Letters 19, 700 (1967); Phys. Rev. 177, 952 (1969).

[2]J. E. Gulley, B. Silbernagel, and V. Jaccarino, J. Appl. Phys. 40, 1318 (1969).

[3]George Reiter, Solid State Commun. 7, 1327 (1969).

[4]C. G. Windsor, Proc. Phys. Soc. (London) 91, 353 (1967); *Neutron Inelastic Scattering* (IAEA, Vienna, 1968); C. G. Windsor, G. A. Briggs, and M. Kestigan, J. Phys. C 1, 940 (1968).

[5]A. Tucciarone, J. M. Hastings, and L. M. Corliss, Phys. Rev. Letters 26, 257 (1971).

[6]P. de Gennes, J. Chem. Phys. Solids 4, 223 (1958).

[7]H. Mori and K. Kawasaki, Progr. Theoret. Phys. (Kyoto) 27, 529 (1962).

[8]R. E. Watson, M. Blume, and G. H. Vineyard, Phys. Rev. 181, 811 (1969).

[9]F. Carboni and P. M. Richards, Phys. Rev. 177, 889 (1969).

[10]H. S. Bennett and P. C. Martin, Phys. Rev. 138, 607 (1965).

[11]P. Resibois and M. DeLeneer, Phys. Rev. 152, 305 (1966); 152, 318 (1966); 178, 806 (1969); 178, 819 (1969).

[12]F. Wegner, Z. Physik 216, 433 (1968); 218, 260 (1969).

[13]A. Erdelyi, W. Magnus, F. Oberhettinger, and F. G. Tricomi, *Higher Transcendental Functions* (McGraw-Hill, New York, 1953), Chap. 11.

[14]W. Marshall and R. D. Lowde, Rept. Progr. Phys. 31, 705 (1968).

[15]R. Stinchcombe, G. Horwitz, F. Englert, and R. Brout, Phys. Rev. 130, 155 (1963).

[16]R. Brout, Phys. Rev. 118, 1009 (1960); 122, 469 (1961).

[17]D. N. Bogolyubov and S. V. Tyablikov, Dokl. Akad. Nauk USSR 126, 53 (1959) [Sov. Phys. Doklady 4, 589 (1959)].

[18]S. V. Tyablikov, Ukrain. Nat. Zhvr. 11, 287 (1959).

[19]G. F. Reiter, thesis (Stanford University, 1968) (unpublished).

[20]V. G. Vaks, A. I. Larkin, and S. A. Pikin, Zh. Eksperim. i Teor. Fiz. 53, 281 (1968) [Sov. Phys. JETP 26, 188 (1968)].

[21]M. Blume and J. Hubbard, Phys. Rev. B 1, 3815 (1970).